Investigation of surface acoustic wave fields in silicon crystals by x-ray diffraction: A dynamical theory approach

R. Tucoulou,[a] O. Mathon, and C. Ferrero
European Synchrotron Radiation Facility (ESRF), BP 220, 38043 Grenoble CEDEX 9, France

V. Mocella
Consiglio Nazionale delle Ricerche-Istituto per la Microelettronica e Microsistemi (CNR-IMM), via P. Castellino 111, 80131 Napoli, Italy

D. V. Roshchupkin
Institute of Microelectronics Technology Russian Academy of Science (RAS), 142432 Chernogolovka, Moscow district, Russia

R. E. Kumon
Department of Physics, University of Windsor, 401 Sunset Avenue, Windsor, Ontario N9B 3P4, Canada

(Received 16 November 2004; accepted 15 March 2005; published online 23 May 2005)

X-ray diffraction spectra at different x-ray energies from a Si crystal subjected to a deformation produced by surface acoustic wave propagation have been modeled using the general framework of dynamical diffraction theory. The simulations have been successfully compared with the corresponding experimental results confirming the accuracy of the elastic model describing the acoustic wave fields inside the crystal. © *2005 American Institute of Physics*.
[DOI: 10.1063/1.1905778]

I. INTRODUCTION

X-ray diffraction has been found to be a powerful tool to characterize surface acoustic wave (SAW) fields in crystals owing to its high sensitivity to the propagation of these waves. High-quality experimental data have already been collected in the case of classical Rayleigh-type SAWs.[1–4] It has been shown that a simple model based on the kinematical approximation could be used sometimes to determine some acoustic parameters from hard x-ray diffraction data. As expected, the kinematical approximation describes well the diffraction process if the crystal is far from being perfect. When the x-ray penetration depth is much smaller than the layer where the acoustic deformation is confined to, x-rays interact only with the deformed part of the crystal. In such a case the kinematical approximation is good and allows the numerical description of the Rayleigh acoustic wave field in the crystal to be validated with sufficient accuracy or simply the acoustic amplitude and penetration depth to be determined in a straightforward manner.[4,2] Unfortunately, this criterion is not satisfied in many practical cases, especially when Si crystals are considered, as in this work. Kinematical theory cannot be applied at small acoustic amplitudes when the crystal can still be considered as perfect. Even in the case of stronger acoustic fields, x-rays might interact with deep undistorted crystal regions. In both cases numerical simulations based on dynamical diffraction theory are needed to precisely analyze the diffraction spectra and for providing quantitative information about the SAW field inside the crystal.

A first paper on diffraction by ultrasonically excited Si crystals was already published presenting solely experimental data.[3] It was indicated that high-resolution x-ray diffraction could be used to "follow" the generation and propagation of a Rayleigh SAW in a Si crystal. In this work we present a model based on the x-ray dynamical theory allowing a quantitative analysis of the parameter characterizing the acoustic wave field in a very large acoustic amplitude range.

II. ACOUSTICS

SAWs propagating on nonpiezoelectric substrates can be used for the development of devices combining acoustical, optical, and semiconductor microelectronic functions in a monolithic form on a compatible substrate. A piezoelectric film covering a transducer is a well-known method for generating a SAW on nonpiezoelectric substrates and ZnO is considered as one of the most efficient materials for this purpose. It can be readily deposited on a wide variety of substrates as an oriented crystalline material of high acoustic coupling efficiency.

The sample used in this experiment was similar to the one described by Tucoulou *et al.*[3] A 1.5-μm ZnO layer was deposited on a Si (001) substrate, covering an interdigital transducer (IDT) which generated a 10-μm wavelength SAW in the ZnO layer. The traveling SAW is initially excited in the piezoelectric layer (by supplying the IDT with a f = 365-MHz sinusoidal voltage) and is then transmitted through the Si crystal propagating along the [110] direction. The acoustic amplitude at the surface can be adjusted from zero to a few angstroms by varying the voltage supplied to the transducer (0–10 V). The relationship between the acoustic amplitude and the voltage is assumed to be linear.

However, the proportionality coefficient between the acoustic amplitude and the applied voltage is not known, and

[a]Electronic mail: tucoulou@esrf.fr

TABLE I. Parameters for Eq. (1) for the direction [100] in (001) cut of crystalline silicon.

Parameter Z	$\mathrm{Re}\,Z+i\,\mathrm{Im}\,Z$	$\lvert Z\rvert\exp(i\phi)$
ζ_1	$-0.4038-0.5312i$	$0.6673\exp(-2.2208i)$
ζ_2	$0.4038-0.5312i$	$0.6673\exp(-0.9208i)$
ζ_3	$-0.3435+0.000i$	$0.3435\exp(3.1416i)$
$\beta_{1.}^{(1)}$	$0.6035-0.2976i$	$0.6729\exp(-0.4582i)$
$\beta_{1.}^{(2)}$	$-0.6035-0.2976i$	$0.6729\exp(-2.6834i)$
$\beta_{1.}^{(3)}$	$0.0000+0.0000i$	$0.000\exp(-0.000i)$
$\beta_{2.}^{(1)}$	$0.0000+0.0000i$	$0.000\exp(-0.000i)$
$\beta_{2.}^{(2)}$	$0.0000+0.0000i$	$0.000\exp(-0.000i)$
$\beta_{2.}^{(3)}$	$0.0000+0.0000i$	$0.000\exp(-0.000i)$
$\beta_{3.}^{(1)}$	$0.4018-0.8145i$	$0.9082\exp(-1.1125i)$
$\beta_{3.}^{(2)}$	$0.4018+0.8145i$	$0.9082\exp(1.1125i)$
$\beta_{3.}^{(3)}$	$0.0000+0.0000i$	$0.000\exp(0.000i)$

therefore the real value of the acoustic amplitude on the crystal is a parameter, which has to be determined numerically.

As described by Royer and Dieulesaint,[5] for example, the displacement components u_i of surface acoustic waves in the linear approximation propagating in a crystal of cubic symmetry can be written in the form

$$u_j/u_0 = \sum_{s=1}^{3} \beta_j^{(s)} e^{i\zeta_s kx_3} e^{i(kx_1-\omega t)}, \tag{1}$$

where $j=1,2,3$, x_1 is the spatial coordinate in the direction of the wave vector, x_3 is the spatial coordinate perpendicular to the surface (positive above the surface), t is the time coordinate, k is the wave number, ω is the angular frequency, ζ_s are the decay coefficients, $\beta_j^{(s)}$ are the amplitude coefficients, and u_0 is a characteristic displacement. One should note that ζ_r and the $\beta_j^{(s)}$ are generally complex-valued constants determined from solving the secular equation subject to stress-free surface boundary conditions.[6] The $\beta_j^{(s)}$ are normalized such that $u_1^2+u_2^2+u_3^2=u_0^2$. To solve for the unknown constants in Eq. (1), it is necessary to input several material parameters. For the results described below, the following second-order elastic moduli from Hearmon[7] were used for silicon: $c_{11}=165$ GPa, $c_{12}=64.0$ GPa, $c_{44}=79.2$ GPa.

Results are given in Table I for the (001) cut of a silicon crystal with a direction of propagation [011]. Surface acoustic waves in this direction are confined to the sagittal plane $[\beta_2^{(s)}=0]$, and the principal axis of the surface particle trajectory is perpendicular to the free surface. Note also that the nonzero real parts of ζ_1 and ζ_2 mean that the surface wave components oscillate as a function of depth in addition to their decay. Let us define $H_0=[\beta_3^{(1)}+\beta_3^{(2)}+\beta_3^{(3)}]u_0^2$ (see Table I) to be the amplitude at the surface $x3=0$ of the component perpendicular to the surface.

In the case of symmetric Bragg reflection geometry, in-plane displacements of the crystal lattice do not influence x-ray Bragg diffraction. By straightforward calculations from Eq. (1), the SAW component normal to the surface u_3 is given by

$$u_3 = |\beta_3^{(1)}| e^{-\zeta_{1i}kx_3} 2\cos(\phi_\beta + \zeta_{1r}kx_3) e^{ikx_1}, \tag{2}$$

where ζ_{1r} and ζ_{1i} are the real and imaginary parts of ζ and ϕ_β the phase of $\beta_3^{(1)}$. A crystalline lattice excited by a SAW can be seen as a periodical grating. X-rays diffracting on deformed atomic planes are sensitive to the grating periodicity and produce by constructive interference some diffraction satellites around the Bragg peak. The angle between adjacent satellites measured on a rocking curve depends on the acoustic wavelength and can be easily calculated starting from the grating equation[3]

$$\delta\theta = \lambda/2\Lambda \sin\theta_B = d_{hkl}/\Lambda. \tag{3}$$

where λ is the x-ray wavelength, Λ is the acoustic wavelength, θ_B is the Bragg incident angle, and d_{hkl} is the interplanar spacing of the considered reflection.

Actually, the grating extends only in a near-surface region characterized by the acoustic penetration depth μ_{ac}^{-1}, which can be expressed from Eq. (2) as the product $k\zeta_{1i}$. Again, the interaction of x-rays with a surface acoustic wave depends strongly on the ratio between the acoustic penetration depth μ_{ac}^{-1} and the x-ray extinction length, the latter determining the region of crystal that significantly contributes to the diffraction process. A simplified model taking into account this relation has been introduced in a previous paper on the base of a kinematical model.[2]

III. DYNAMICAL SIMULATIONS

Several dynamical theory models describing the effects of acoustic wave fields on x-ray diffraction spectra have already been published. Most of them deal, however, only with bulk acoustic waves,[8,9] or with SAWs but without any comparison with experimental data.[10,11]

Recently some of us have published a paper showing that rocking curves of a SAW excited $LiNbO_3$ crystal can be well simulated by using a dynamical theory model.[12] The aim of this paper is to present the results of an additional investigation for a crystal of a nonpiezoelectric material such as Si and to assess the degree of accuracy of the simulation in the quantitative analysis of acoustic wave fields in such crystals.

The dynamical theory (DT) describes exactly the x-ray diffraction for a perfect crystal.[13] In the case of a deformed crystalline lattice the Takagi–Taupin (TT) equations have proven to provide a particularly powerful formalism that generalizes the dynamical diffraction theory describing the propagation of x-rays in a crystal with an arbitrary deformation.[14–16]

Strictly speaking, DT and the TT equations hold for a crystal at rest, without considering temporal variations. This is entirely justified in the case of ultrasonic acoustic waves where the period of the acoustic wave $\tau_{\mathrm{ac}}=1/\omega_{\mathrm{ac}}$ is of the order of 10^{-8} s.

This period is much longer than the characteristic time of x-ray diffraction, τ_{rx}, that can be expressed as the ratio between the extinction length projected along the direction of propagation and the propagation speed c of light (*extinction depth transversal time*):[17,18]

$$\tau_x = \frac{\Lambda_{\text{ext}}}{c\gamma_0},$$

where Λ_{ext} is the x-ray extinction length for the considered reflection and γ_0 is the cosine of the angle between the incident direction and the normal to the crystal. In our case $\tau_{\text{rx}} \approx 10^{-13} \ll \tau_{\text{ac}}$.

One can thus consider the deformation as static in comparison with the time scale of the diffraction process. This justifies the use of the classical dynamic theory and its generalization by the TT equations, without resort to their time-dependent extension, which can instead be useful when the deformation has more rapid temporal variations, as in the case of optical phonons.[19]

Hence, we consider the TT equations,[14–16] simplified for the case of a Bragg symmetric reflection, like that we consider in the experiment:

$$\begin{cases} \dfrac{\partial D_0}{\partial s_0} = -i\pi k \chi_{-h} D_h(\mathbf{r}) \\ \dfrac{\partial D_h}{\partial s_h} = -i\pi k \chi_h D_0(\mathbf{r}) + 2\pi i k \beta'(\mathbf{r}) D_h(\mathbf{r}) \end{cases}$$

$$\beta'(\mathbf{r}) = -(\theta - \theta_B)\sin(2\theta_B) - \frac{1}{k}\frac{\partial(\mathbf{hu})}{\partial s_h}, \tag{4}$$

where s_0 and s_h are the coordinates along the forward and diffracted directions, respectively, χ_h and χ_{-h} are the components of the Fourier expansion of the dielectric susceptibility, $k=1/\lambda$, $\mathbf{h}$ is the diffraction vector, $\mathbf{u}$ is the displacement vector. D_0 and D_h are the forward and diffracted wave fields, respectively. $\theta-\theta_B$ is the angular deviation from the Bragg law and $\mathbf{r}=(s_0, s_h)$ is the space variable in the diffraction plane.

For the simulations presented in this study, Eq. (4) were solved numerically[20] by inserting the displacement $\mathbf{u}$ produced by the acoustic waves calculated from Eq. (2) for each value of the angle θ. As mentioned above, $\mathbf{u}$ can be restricted to u_3.

Because the incident wave on the crystal is monochromatized by the Si (333) reflection, it is well justified to consider the incident wave as a coherent monochromatic plane wave. The angular beam divergence delivered by the Si (333) crystal is accounted for by convolving the wave angular profile with the Si (333) reflectivity curve, assuming this as perfect. Furthermore, in this case there is no crystal analyzer that would require the discrimination of the diffracted directions from the vibrating crystal by means of a suitable Fourier analysis,[21] therefore the intensity recorded by the detector is obtained as

$$I_h(\theta) = \int_{-\infty}^{+\infty} |D_h(x,\theta)|^2 dx, \tag{5}$$

where $D_h(x,\theta)$ is the solution of the numerical integration of Eq. (3) along the entrance surface x, for a given incident angle θ. The absence of an analyzer implies that the intensity in Eq. (5) corresponds to all the diffracted directions from the vibrating crystal. For Parseval's theorem this intensity is equivalent to the total intensity on the crystal in the direct space.

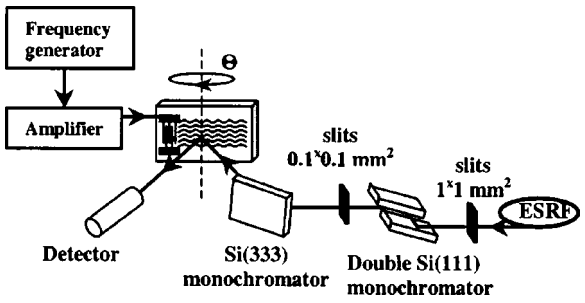

FIG. 1. Experimental layout.

IV. EXPERIMENT

The experiment described in this paper was carried out using a double axis x-ray diffractometer on the optics beamline (BM05) at the ESRF (see Fig. 1).

The x-ray energy was selected by a standard double Si(111) monochromator slightly detuned to remove higher harmonics. A second Si(333) monochromator was placed directly in front of the vibrating Si(400) crystal to improve the monochromaticity down to $\Delta\lambda/\lambda \approx 10^{-6}$ which is much smaller than $\Delta\lambda/\lambda \approx 10^{-5}$ accepted by the vibrating crystal. Primary and secondary slits with horizontal and vertical gaps of 1×1 and 0.1×0.1 mm, respectively, were used to collimate the beam. The dimensions of the crystal surface illuminated by the x-ray beam gave the spatial resolution of the measurement. The double axis diffractometer can provide an angular resolution of $\sim$0.1 arc sec, which is sufficient to separate the diffraction satellites of the rocking curve. A Cyberstar NaI scintillation counter was used to measure the diffracted intensity.

The x-ray beam hits the Si surface far from the ZnO film to make sure that the probed SAW propagated in a free elastic regime.

It should be noticed that in Ref. 3, rocking curves were measured after a Si (333) analyzer. This analyzer has been removed for the present experiment to measure the actual profile of each diffraction satellite. Resolution was still good enough to avoid overlap between the satellites.

V. RESULTS

In order to evaluate the accuracy of the acoustical model we have used, it was decided to remain at a fixed x-ray energy and to vary the acoustic amplitude H_0 by varying the voltage amplitude supplied to the interdigital transducer. Figure 2 shows several rocking curves measured at 14 keV and at voltages of 10, 20, 40, and 60 mV. The model can be validated only if all the rocking curves can be fitted with the same numerical acoustical parameters except the acoustic amplitudes H_0, which should remain proportional to the supplied voltages. The number of satellites N increases with the amplitude following approximately the law $N \approx 2\pi H_0/d$ and does not depend on the x-ray energy.[3] This equation allows us to restrict the amplitude range to be tested by the simula-

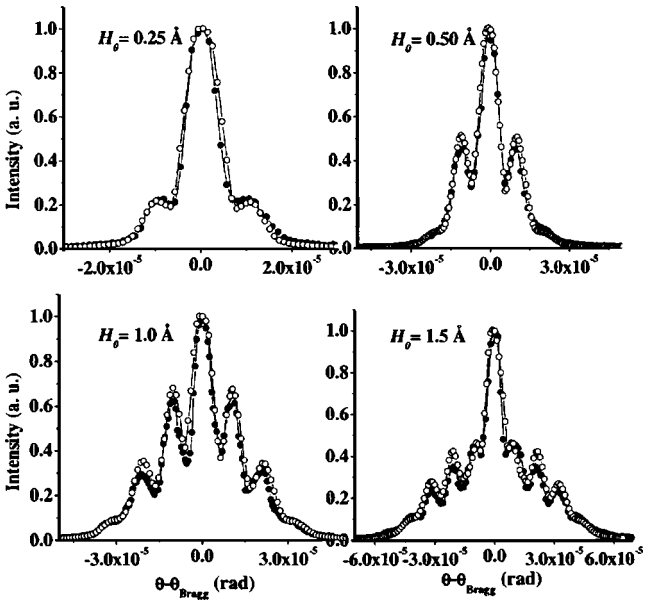

FIG. 2. Measured (filled circles) and calculated (unfilled circles) rocking curves at various acoustic amplitudes. $E=14$ keV, $\Lambda=13$ μm.

tion to approximately 0.22 Å in the case of Si(400) by simply counting the number of satellites on the rocking curve to be simulated.

All the theoretical rocking curves in Fig. 2 have been calculated using Eq. (2) and by simply adjusting H_0 to obtain a reasonable agreement with the measured data. Both calculated acoustic amplitudes and voltages supplied to the transducer follow the same linear variation.

To estimate the precision of the calculations, one can see in Fig. 3 ($H_0=1$ Å, $E=14$ keV) that an acoustic amplitude variation of 0.1 Å introduces already a clear mismatch between the measured and calculated rocking curves. The effect of the variation of the acoustic amplitude is the most visible in the region of the rocking curve where the highest-order satellites grow up. Concerning the acoustic penetration depth, the accuracy of the simulation is of the order of 0.5 μm, as this can be noted in Fig. 4.

Another possible way of verifying the accuracy of the

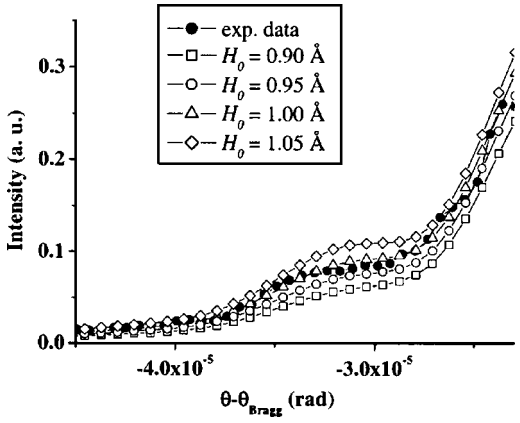

FIG. 3. Measured and calculated rocking curves for several acoustic amplitudes at fixed acoustic penetration depth $\mu_{ac}^{-1}=k\zeta_{1i}$. Relative to the $H_0=1$ -Å curve in Fig. 1, the scale is zoomed in on the angular range where the highest-order satellite is growing.

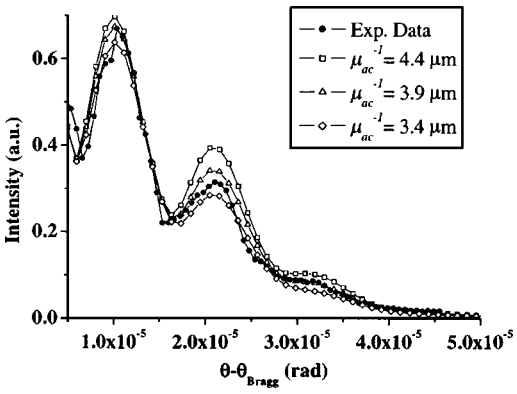

FIG. 4. Measured and calculated rocking curves for several acoustic penetration depths at fixed acoustic amplitude $H_0=1$ Å.

acoustical model adopted in the simulations is to study one sample excited by a wave of constant ultrasonic amplitude and frequency and to vary only the x-ray energy. The results of the calculations should always converge to the same acoustical parameters regardless of the x-ray energy. Figure 5 shows the rocking curves measured and simulated at constant amplitude $H_0=1$ Å and at x-ray energies 14, 18, and 25 keV. It can be seen that the agreement between the experiment and theory does not change over the whole energy range. It also shows that in the case of Si crystals, the x-ray energy (at least in the range of 14–25 keV) is not a critical

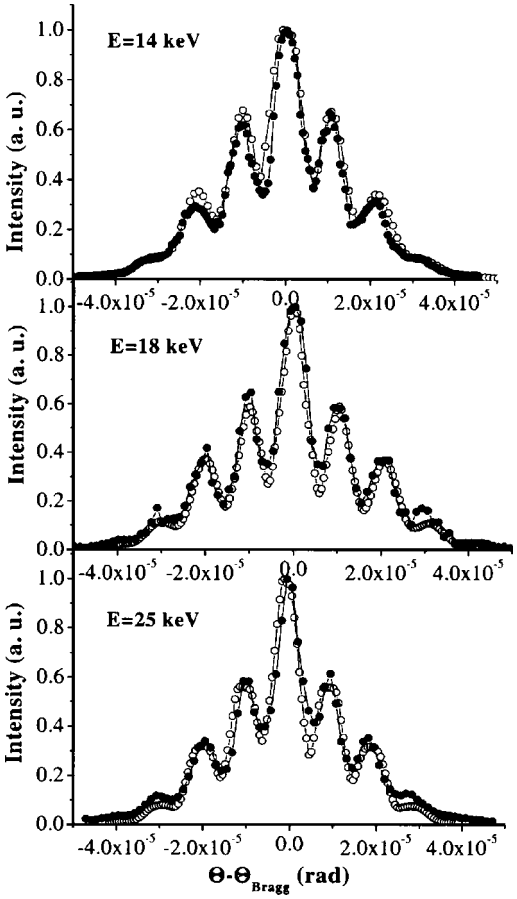

FIG. 5. Measured (filled circles) and calculated (unfilled circles) rocking curves at three different energies. Calculations are performed with $\Lambda=13$ μm, $H_0=1$ Å, and $\mu_{ac}^{-1}=k\zeta_{1i}=3.9$ μm.

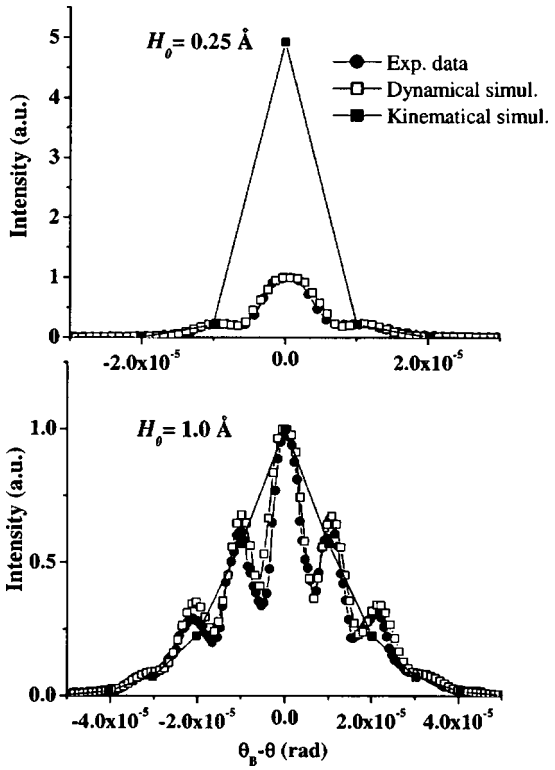

FIG. 6. Comparison of kinematic and dynamic calculations for two different acoustic amplitudes. $E=14$ keV, $\Lambda=13$ μm. For the kinematic calculation, only the maximum intensity is given for each satellite, the line being only a guide for the eyes.

parameter to probe the acoustic wave field. Owing to the order of magnitude of μ_{ac}^{-1}, x-rays in the range of 14–25 keV can easily pass through the whole acoustically excited layer of the crystal.

In the case of heavier materials with absorption edges in the available energy range ($LiNbO_3$, Langasite crystals, for example), the anomalous region should be of course avoided. Nevertheless, as soon as absorption edges can be reached with x-rays, some strong variations in the x-ray penetration depth can be obtained by tuning the energy around the edge. This allows introducing some selectivity in the depth of the crystal layer probed by x-rays.

It is interesting to compare dynamical and kinematical simulations.[2] As shown in Fig. 6 ($E=14$ keV, $\Lambda=13$ μm), dynamical simulations give much better results irrespectively of the acoustic amplitude. In the kinematical case, the higher the acoustic amplitude the better the simulations are [provided the analytical description (1) of the Rayleigh wave is still valid]. As the acoustic amplitude increases, the dynamical diffraction regime evolves into a kinematical one, and therefore kinematical simulations become more and more reliable. In Ref. 4 where the x-ray penetration depth is of the order of 1 μm, kinematical simulations give good results.

VI. CONCLUSION

A computational method has been developed and tested to estimate the fundamental parameters describing the surface acoustic wave field propagating in a ZnO/Si (001)-layered structure.

The approach described in this work is clearly more powerful than the kinematical one proposed in Refs. 2 and 4 because it is derived directly from the x-ray dynamical diffraction theory by means of the TT equations for a two-beam case. No approximation of any kind has been introduced in the x-ray diffraction model. The coupling with the acoustical model is accounted for in the deformation term of the TT equations, which have to be solved numerically inasmuch as no analytical solution exists for a displacement like that in Eq. (1). As far as Eq. (1) holds true for the acoustic amplitudes, our model enables us to simulate correctly the diffraction profiles, and not just predict the peak intensity point values (as it was the case in Ref. 2) for a wide range of acoustic deformations: up to at least 70% of the atomic d spacing.

The classical description of the Rayleigh acoustic wave has been confirmed to be very accurate, as anticipated. The next step would be to study more complicated cases like pseudo-SAWs,[6] dispersive SAWs in thin-film systems,[22] or nonlinear SAWs[23,24] to characterize the accuracy of the acoustical models generally used in these specific situations.

[1] W. Sauer, M. Streibl, T. H. Metzger, A. G. C. Haubrich, S. Manus, A. Wixforth, and J. Peisl, Appl. Phys. Lett. **75**, 1709 (1999).
[2] R. Tucoulou, F. de Bergevin, O. Mathon, and D. V. Roshchupkin, Phys. Rev. B **64**, 134108 (2001).
[3] R. Tucoulou, O. Mathon, R. Pascal, D. V. Roshchupkin, I. A. Schelokov, E. Cattan, and D. Remiens, J. Appl. Crystallogr. **33**, 1019 (2000).
[4] D. V. Irzhak, D. V. Roshchupkin, R. Tucoulou, O. A. Buzanov, and S. A. Sakharov, J. Appl. Phys. **94**, 6692 (2003).
[5] D. Royer and E. Dieulesaint, *Ondes élastiques dans les solides* (Masson, Paris, 1999).
[6] G. W. Farnell, in *Physical Acoustics*, edited by W. P. Mason and R. N. Thurston (Academic, New York, 1970), Vol. 6, pp. 109–166.
[7] R. F. S. Hearmon, in *Elastic, Piezoelectric, Pyroelectric, Piezooptic, Electrooptic Constants and Nonlinear Dielectric Susceptibilities of Crystals*, Landolt-Bornstein New Series Group III Vol. 11, edited by K. H. Hellwege and A. M. Hellwege (Springer, New York, 1979), pp. 1–244.
[8] R. Köhler, W. Möhling, and H. Peibst, Phys. Status Solidi B **61**, 173 (1974).
[9] I. R. Entin and K. P. Assur, Acta Crystallogr., Sect. A: Cryst. Phys., Diffr., Theor. Gen. Crystallogr. **37**, 769 (1981).
[10] I. Polikarpov and E. Zolotoyabko, J. Phys. D **30**, 2591 (1997).
[11] R. Colella, Z. Naturforsch. A **37**, 437 (1982).
[12] I. A. Schelokov, D. V. Roshchupkin, D. V. Irzhak, R. Tucoulou, J. Appl. Crystallogr. **37**, 52 (2004).
[13] A. Authier, *Dynamical Theory of X-Ray Diffraction*, (Oxford University Press, London, 2001).
[14] S. Takagi, Acta Crystallogr. **15**, 1311 (1962).
[15] S. Takagi, J. Phys. Soc. Jpn. **26**, 1239 (1969).
[16] D. Taupin, Bull. Soc. Fr. Mineral. Cristallogr. **87**, 469 (1964).
[17] F. Chukhowskii and E. Förster, Acta Crystallogr., Sect. A: Found. Crystallogr. **A51**, 668 (1995).
[18] J. S. Wark and R. Lee, J. Appl. Crystallogr. **32**, 692 (1999).
[19] P. Sondhauss and J. S. Wark, Acta Crystallogr., Sect. A: Found. Crystallogr. **A59**, 7 (2003).
[20] Y. Epelboin, V. Mocella, and A. Soyer, Philos. Trans. R. Soc. London, Ser. A **357**, 2739 (1999).
[21] V. Mocella, W.-K. Lee, G. Tajiri, D. Mills, C. Ferrero, and Y. Epelboin, J. Appl. Crystallogr. **36**, 129 (2003).
[22] G. W. Farnell and E. L. Adler, in *Physical Acoustics*, edited by W. P. Mason and R. N. Thurston (Academic, New York, 1972), Vol. 9, pp. 35–127.
[23] R. E. Kumon and M. F. Hamilton, J. Acoust. Soc. Am. **111**, 2060 (2002).
[24] R. E. Kumon and M. F. Hamilton, J. Acoust. Soc. Am. **113**, 1293 (2003).